First-principles calculations for coefficients of the isobaric mass multiplet equation in the fp shell

W. E. Ormand,[1] B. A. Brown,[2] and M. Hjorth-Jensen[2,3]

[1] *Lawrence Livermore National Laboratory, Livermore, CA 94551, USA*
[2] *Department of Physics and Astronomy and National Superconducting Cyclotron Laboratory, Michigan State University, East Lansing, MI 48824-1321, USA*
[3] *Department of Physics, University of Oslo, N-0316, Oslo, Norway*

We present the first calculations for the c-coefficients of the isobaric mass multiplet equation (IMME) for nuclei from $A = 42$ to $A = 54$ based on input from several realistic nucleon-nucleon interactions. We show that there is clear dependence on the short-ranged charge-symmetry breaking (CSB) part of the strong interaction. There is a significant variation in the CSB part between the commonly used CD-Bonn, N^{3}LO and Argonne V18 nucleon-nucleon interactions. All of them give a CSB contribution that is too large when compared to experiment.

PACS numbers: 21.30.Fe, 21.60.Cs, 21.60.De, 27.40.+z

Isospin is a powerful spectroscopic tool in nuclear physics that can be used to label and characterize states not only in a specific nucleus, but also corresponding states in an analog nucleus. Isospin, denoted by T, is an additive quantity similar to the intrinsic spin of the proton and neutron. The charge, Q, of the particle is defined by the z-component via $Q = \frac{1}{2} + T_z$. Thus, for a nucleus with Z protons and N neutrons, the z-component is $T_z = (Z-N)/2$, and a nucleus may have isospin states with $T \geq T_z$, Isospin symmetry is broken by components in the nuclear Hamiltonian that treat protons and neutrons differently. The most obvious, and significant, component is the Coulomb interaction acting only between protons due to their electric charge. There are, however, weaker isospin-symmetry breaking components in the nucleon-nucleon interaction itself caused by differences in the masses of up and down quarks and their intrinsic electric charges, which is reflected in the slightly different masses exhibited by neutrons and protons [1] and the slightly different strong-interaction scattering lengths observed in the proton-proton (pp), neutron-neutron (nn), and the $T = 1$ proton-neutron (pn) channels.

Important signatures of isospin-symmetry breaking interactions are differences in the binding energy of nuclei within the same isospin multiplet with fixed nucleon number A. These mass splittings, or Coulomb-displacement energies offer a sensitive probe of the properties of isospin-symmetry breaking in nuclei. The three $T = 1$ nucleon-nucleon channels can be decomposed into three isospin components: isoscalar (rank 0), isovector (rank 1), and isotensor (rank 2), defined in terms of the pp, nn, and pn interactions via

$$v^{(0)} = \frac{1}{3}(v_{pp} + v_{nn} + v_{pn}) \quad (1)$$

$$v^{(1)} = (v_{pp} - v_{nn}) \quad (2)$$

$$v^{(2)} = v_{pn} - \frac{1}{2}(v_{pp} + v_{nn}). \quad (3)$$

With these three components, the masses for a set of states within a multiplet with isospin T may be described by the isobaric mass multiplet equation (IMME)

$$M(T_z) = a + bT_z + cT_z^2, \quad (4)$$

where the coefficients a, b, and c are dependent on the isoscalar, isovector, and isotensor components of the nuclear Hamiltonian, respectively. The linear and quadratic dependence on T_z is due to the application of the Wigner-Ekhart theorem and the appropriate Clebsch-Gordon coefficients arising for the isovector and isotensor components of the Hamiltonian, respectively.

In this letter, we compute Coulomb-displacement energies as a function of excitation for nuclei in the mass range $42 \leq A \leq 54$ using the isospin-symmetry breaking interactions derived from realistic nucleon-nucleon interactions. Here, we focus on the effects of the isotensor component as exhibited in the c-coefficient of the IMME.

We performed a series of shell-model calculations using the program BIGSTICK to compute the c-coefficients of the IMME for $1p0f$-shell nuclei with $42 \leq$ A ≤ 54. The pertinent effective interactions for the degrees of freedom of the $1p0f$ shell were derived using many-body perturbation theory, see for example Ref. [4]. The two-body matrix elements where computed in two steps, first by renormalizing the nuclear two-body interactions using both a G-matrix approach and the so-called V$_{lowk}$ method. For the nuclear interactions, we employed the realistic N^{3}LO [5], AV18 [6] and CD-Bonn [7] nucleon-nucleon interactions. These interaction models allow for the breaking of isospin symmetry and charge symmetry and include the isotensor and isovector components of the strong interaction. The reader should note that the AV18 interaction model includes electromagnetic corrections and the full model is used when renormalizing the short-range part of the force. This may lead to slightly different Coulomb interactions in a finite nucleus. The renormalized nucleon-nucleon interactions were computed using a harmonic oscillator basis with an oscillator energy $\hbar\omega = 10.5$ MeV with an effective Hilbert space defined

by the first twelve oscillator shells. The G-matrix and V_{lowk} interactions were obtained with a cut-off parameter of $\Lambda = 2.1$ fm^{-1}. For the N^{3}LO and the CD-Bonn interactions, the Coulomb interaction was added after the renormalization process. The second step consisted in obtaining an effective interaction tailored to a small shell-model space. This was achieved using many-body perturbation theory up to third order in the renormalized nucleon-nucleon interactions, including so-called folded diagrams [4]. All codes used to generate these interactions are publicly available [8]. The renormalization was performed with and without the Coulomb interaction, and the Coulomb two-body matrix elements were obtained from the difference between these proton-proton (pp) matrix elements. The renormalized interaction computed without Coulomb was then decomposed into the three isospin components: isoscalar (rank 0), isovector (rank 1), and isotensor (rank 2), as defined in Eqs. (1)-(3).

The c-coefficients of the IMME were obtained utilizing first-order perturbation theory. The base for each calculation was the eigenstate, E_0 for each member of the $T = 1$ triplet, $|T_z\rangle$, obtained using the isoscalar GX1A Hamiltonian [9]. The GX1A interaction was used instead of the $v^{(0)}$ interaction obtained from the realistic interaction described above because of well-known extensions that must be included to properly capture the behavior of higher-order components and the three-body interaction in the traditional configuration-interaction shell model for atomic nuclei, see for example Refs. [11, 12]. The expectation value of the Coulomb, isovector, and isotensor interactions are then computed to give the full energy for each state,

$$E(T_z) = E_0 + \langle T_z | v^{\rm Coul} + v^{(1)} + v^{(2)} | T_z \rangle$$

and the c-coefficient is then computed from

$$c = [E(T_z = 1) - 2E(T_z = 0) + E(T_z = -1)]/2.$$

The A-dependence was properly accounted for by scaling the Coulomb matrix elements by $\sqrt{\hbar\Omega(A)/10.5}$, while the isovector and isotensor interactions were assumed to have the same A-dependence as the GX1A interaction. For each A-value, $\hbar\Omega(A)$ was determined by reproducing the *rms* radius obtained from a Hartee-Fock calculation for $42 \leq A \leq 54$ nuclei using the SkX Skyrme interaction [10].

Figure 1 shows the results CD-Bonn to first, second and third order in many-body perturbation theory. The contributions are divided into Coulomb (full lines) and CSB (dashed lines). The J-dependence of these two contributions is very different. The long-range Coulomb has a relatively flat J-dependence with only a small rise at $J = 0$. The CSB contribution at $A = 42$ shows a peak at $J = 0$ with a sharp drop towards $J = 2$, which is characteristic of a short-ranged interaction. This pattern is observed if one employs a simple δ-function interaction model.

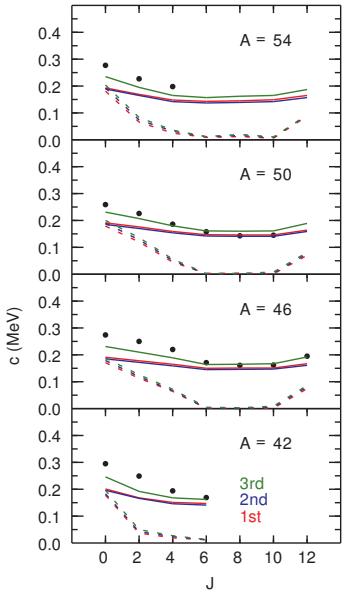

FIG. 1. (color online) Results for the CD-Bonn potential in 1$^{\rm st}$, up to 2$^{\rm nd}$ and up to 3$^{\rm rd}$ order. The black circles are the experimental data. The solid lines show the Coulomb contribution, and the dashed lines show the CSB contribution.

For $A = 42$, $J = 6$ is the maximum angular momentum (for $T = 1$) in the $1p0f$ model space. For higher values of A, this sharp drop at $J = 2$ is replaced by a linear drop to $J = 6$ due to configuration mixing. We note that for $J = 8$ and 10, the effect of charge-symmetry breaking is small. The experimental data is taken from the compilation [2], except for $A = 46$, where we use the results from Fig. 2 of [3].

Both Coulomb and CSB have a small increase at $J = 12$. The reason for this is that protons with $J = 6$ and neutrons with $J = 6$ are maximally aligned, resulting in an enhancement of the overlapping proton and neutron density distributions.

The CSB contribution turns out to be almost order independent, while the Coulomb contribution is almost the same to first and second order in many-body perturbation theory, but increases by 10-20% to third order. This suggests that the CSB interaction is substantially short-ranged in nature, and the G-matrix and V_{lowk} treatment may be sufficient. A simple analysis of all $J = 0$ two-body matrix elements, using Eqs. (1)-(2), shows that for the core-polarization contribution to second order, the correction to c is about ten times smaller than that for a. This applies to most two-body matrix elements that define Eqs. (1)-(2).

It is remarkable that the experimental data are in rather good agreement with the third order Coulomb result, where there seems to be no need for CSB even

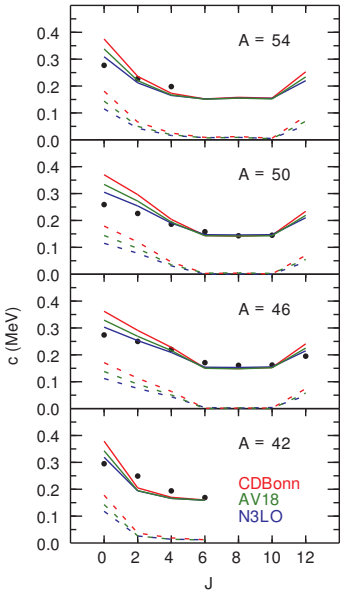

FIG. 2. (color online) 1st order calculations compared to experiment. The black circles are the experimental data. The solid lines show the sum of Coulomb and CSB contributions. The dashed lines show only the CSB contribution.

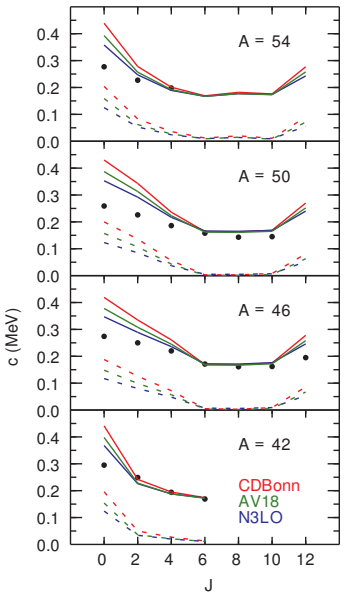

FIG. 3. (color online) Calculations up to 3rd order compared to experiment. See caption to Fig 2.

though this component is well known to be important in nucleon-nucleon (NN) scattering data that is incorporated into the potential models.

Figure 2 shows the results for the three potential models to first order in interaction. This shows that the CSB contribution is model dependent. There could be a few

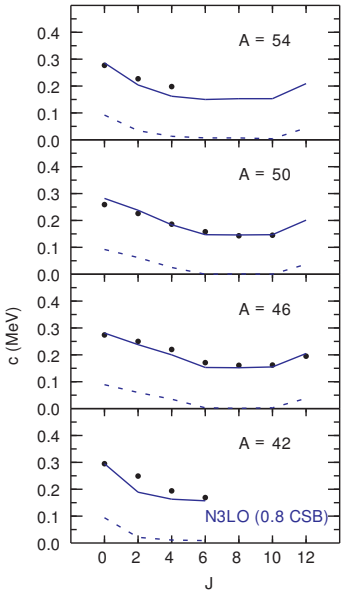

FIG. 4. (color online) 1st order calculations for N^{3}LO with the CSB part multiplied by 0.8 and compared to experiment. See caption to Fig 2.

reasons for this. While the NN interactions are all fit to scattering data and reproduce the proton-neutron scattering length equally well, there could be differences in the underlying treatment of the CSB components. In addition, while AV18 is a purely local potential, both N^{3}LO and CD-Bonn are non-local, albeit in different ways. Finally, the short-range correlation effects taken into account in the G-matrix and V$_{lowk}$ renormalizations could have different effects on this small component of the NN interactions, which may be corrected when induced three-nucleon terms are included. We note that the results obtained with N^{3}LO are in best agreement with experiment, although all three interactions over predict the c-coefficients. This in its own self might be a signature of charge-symmetry breaking in the initial three nucleon interaction.

Figure 3 shows the results for the three potentials to third order.

Our work guides future investigations in directions. For better first principles calculations, one should understand the origin of the different CSB contributions from these three realistic potentials. In particular, in the spirit of using nuclear data to constrain the NN and three-nucleon ($3N$) interactions (in addition to NN scattering data) one should use the c-coefficient as a constraint on the CSB part. From a practical point of view, we start with the fact that first-order Coulomb plus CSB is already close to the data. We can make it almost perfect by taking the first-order Coulomb contribution and add 80% of the N^{3}LO CSB part. This is shown in Fig. 4. The largest deviation from experiment comes for $J = 2$

at $A = 42$. However, $A = 42$ is just at the beginning of the $1p0f$ model space and it is well know that admixtures from core excitations from the $0s - 1d$ shell are very important especially for $J = 0$ and $J = 2$. For example, the 2^+ to 0^+ B(E2) value for ^{42}Ca is about ten times larger in experiment than compared to theory. The experimental fall off from $J = 0$ to $J = 6$ in $A = 42$ looks like calculation for $A = 46$. The theoretical wave functions for A=42 are dominated by $(f_{7/2})^2$ configurations and the wave functions for $A = 54$ are dominated by $(f_{7/2})^{-2}$ configurations. These two configuration have the same spectra (except for a small mass dependence). Compared to $A = 42$ the J dependence observed for $A = 54$ is closer than expected for these pure configurations.

In conclusion, we have presented the first calculations for the c-coefficients of the IMME for nuclei from $A = 42$ to $A = 54$, based on input from several realistic nucleon-nucleon interactions and their pertinent shell-model effective interactions. The CSB contribution is almost independent of the order of renormalization in many-body perturbation theory, suggesting that the charge-symmetry breaking part of the interaction is to a large extent of a short-range nature. In effective field theory this may point to two-pion or higher-pion excitations that probe the short range nature of the CSB interaction. Whether these conclusions remain when three-body interactions are included, given the short-range nature of the CSB part of the interactions, remains to be seen.

BAB acknowledges U.S. NSF Grant No. PHY-1404442. MHJ acknowledges U.S. NSF Grant No. PHY-1404159 and the Research Council of Norway under contract ISP-Fysikk/216699. WEO acknowledges support from the U.S. Department of Energy, Office of Science, Office of Nuclear Physics, under Field Work Proposal No. SCW0498. This work was performed under the auspices of the U.S. Department of Energy by Lawrence Livermore National Laboratory under Contract DE-AC52-07NA27344. Computing support for this work came from the Lawrence Livermore National Laboratory (LLNL) institutional Computing Grand Challenge program.

[1] G. A. Miller, A. K. Opper, and E. J. Stephenson, Annu. Rev. Nucl. Sci. **56**, 253 (2006).
[2] Y. H. Lam, B. Blank, N. A. Smirnova, J. B. Bueb, and M. S. Antony, At. Data and Nucl. Data Tables **90**, 680 (2013).
[3] P. E. Garrett *et al.*, Phys. Rev. Lett. **87**, 132502 (2001).
[4] M. Hjorth-Jensen, E. Osnes, and T. .T. .S. Kuo, Phys. Rep. **261**, 125 (1995).
[5] D. R. Entem and R. Machleidt, Phys. Rev. C **68**, 041001(R) (2003).
[6] R. B. Wiringa, V. G. J. Stoks, and R. Schiavilla, Phys. Rev. C **51**, 38 (1995).
[7] R. Machleidt, Phys. Rev. C **63**, 024001 (2001).
[8] All codes used to generate the effective interactions are available at https://github.com/ManyBodyPhysics/CENS.
[9] M. Honma, T. Otsuka, B. .A. Brown, and T. Mizusaki, Phys. Rev. C **65**, 061301(R) 2002; Euro. Phys. Jour. A **25 Suppl.** 1 499 (2005).
[10] B. A. Brown, Phys. Rev. C **58**, 220 (1998).
[11] A. P. Zuker, Phys. Rev. Lett. **90**, 042502 (2003).
[12] A. Ekström, G. R. Jansen, K. A. Wendt, G. Hagen, T. Papenbrock, B. D. Carlsson, C. Forssen, M. Hjorth-Jensen, P. Navratil, and W. Nazarewicz, Phys. Rev. C **91**, 051301(R) (2015).